horticulturae

MDPI

Article

Comparison of Aroma Components in Different Finger Citron (*Citrus medica* 'Fingered') Leaves Based on HS-SPME-GC-MS, ROAV, and Molecular Docking

Jiaqi Wu [1,†], Yuxin Zhou [2,3,†], Benyi Lu [1], Xiong Lin [1], Yiwen Cao [1], Ping Sun [1], Chenfei Chen [3], Jiansheng Shen [1,*] and Yi Wang [1,*]

[1] Jinhua Laboratory of Biological Seed Industry and Modern Agricultural Machinery, Jinhua Academy of Agricultural Sciences, Jinhua 321000, China
[2] Marine College, Shandong University, Weihai 264200, China
[3] Jinhua Institute of Floriculture and Nursery Industry, Jinhua 321000, China
* Correspondence: sjsjhnky@163.com (J.S.); nazard@163.com (Y.W.)
† These authors contributed equally to this work.

Abstract

Finger citron (*Citrus medica* 'Fingered') is used as a raw material for essential oil extraction due to its distinctive fragrance. Studies have predominantly focused on the fruit, but the aroma components of the leaves have not yet been systematically compared. This study used headspace solid-phase microextraction gas chromatography mass spectrometry combined with the relative odor activity value (ROAV) and molecular docking to analyze the volatile compound composition, aroma characteristics, and interactions with human olfactory receptor OR1A1 in leaves of different finger citron cultivars. Based on pooled samples of six individual plants per cultivar, a total of 394 compounds were tentatively identified among all of the cultivars, with terpenoids being the most abundant class. (+)-Sylvestrene, geranial, and neral were the three components with the highest relative contents. Analysis of the pooled samples preliminarily revealed differences in volatile composition among cultivars. Yunfoshou had the relatively highest total volatile content. The volatile profiles of QingyiTongzi, Xiuzhen, Tianci, Cuiyu, Kaixin, and Guangfoshou were relatively similar to each other but differed from those of Yangguang and Yunfoshou. Thirteen key aroma-active compounds were screened using ROAV analysis, and linalool exhibited the highest ROAV across all of the cultivars. The aroma profiles of all of the cultivars were predominantly floral. Molecular docking predictions showed that the binding energies of the 13 key aroma compounds with OR1A1 ranged from −5.859 to −8.652 kcal/mol, with Asn109 and Tyr258 involved in hydrogen bonding and hydrophobic interactions, respectively. This study preliminarily reveals the aroma characteristics of leaves from different finger citron cultivars and provides a preliminary theoretical basis for finger citron breeding and the development of deep-processed leaf products.

Keywords: Fingered citron leaves; aroma compounds; relative odor activity value (ROAV); molecular docking

Check for updates

Received: 5 August 2026
Revised: 1 October 2026
Accepted: 13 October 2026
Published: 17 October 2026

Copyright: © 2026 by the authors. Licensee MDPI, Basel, Switzerland. This article is an open access article distributed under the terms and conditions of the Creative Commons Attribution (CC BY) license.

1. Introduction

Finger citron (*Citrus medica* 'Fingered'), which belongs to the Rutaceae family, has long been valued in traditional medicine for its therapeutic effects [1–3]. In addition to its medicinal uses, finger citron is cultivated as an ornamental potted plant and a

raw material for essential oil extraction due to its distinctive morphology and refreshing fragrance. Previous studies have demonstrated that essential oil distilled from finger citron fruit is predominantly composed of monoterpenes, such as limonene and γ-terpinene, and exhibits a broad range of bioactivities, including anti-inflammatory, antimicrobial, and antidepressant effects [4–7]. These properties confer application potential in food processing, flavor, and fragrance industries and aromatherapy.

In China, finger citron is mainly cultivated in Zhejiang, Guangdong, Guangxi, Sichuan, and Yunnan provinces, where local cultivars have been developed. Aroma components, which are primarily volatile organic compounds (VOCs), are critical quality indicators and the foundation of essential oil production [8]. In addition to the fruit, leaves are a key organ for volatile compound biosynthesis and accumulation in finger citron, and their aroma composition is closely associated with the overall aroma profile and quality of the plant.

The aroma compound composition and content are jointly regulated by genetic factors and environmental conditions [9,10]. The characteristic fragrance of *Citrus* species arises from the presence of VOCs, including alcohols, aldehydes, ketones, terpenes, and esters [11–13]. Xu et al. analyzed the aroma components of finger citron from different geographical origins using headspace solid-phase microextraction gas chromatography mass spectrometry (HS-SPME-GC-MS), and they found that geraniol and d-limonene influenced their aroma profiles [14]. Specifically, Zhejiang finger citron exhibited pronounced woody and grassy notes, Guangdong finger citron tended to be sweeter, and Yunnan finger citron had floral characteristics [14]. Song et al. compared the volatiles of finger citron pulp and peel using headspace solid-phase microextraction (HS-SPME) and purge-and-trap with Tenax TA adsorbent, revealing a high similarity between the volatile profiles of pulp and peel, with limonene, α-pinene, and β-pinene being the primary aroma contributors [15]. Wei et al. employed solvent-free microwave extraction as a green approach for isolating finger citron essential oil, and they identified d-limonene, γ-terpinene, and α-pinene as the major constituents [16]. However, previous studies have predominantly focused on the fruit, with relatively little comparison of leaf aroma among cultivars and identification of aroma-active compounds.

Although finger citron fruit is a conventional source of essential oil, its irregular shape makes peeling difficult, and using whole fruit for oil extraction reduces material utilization efficiency since oil glands are predominantly located in the peel. In addition to fruit, oil glands are also abundantly distributed in leaves, flowers, and stems [17], rendering the entire plant suitable for essential oil production. Compared to fruit, leaves—as major organs of volatile metabolism—offer advantages in terms of sampling convenience and material availability. Lin et al. compared the essential oils from fruit and leaves of Sichuan finger citron and found 22 common compounds, but their relative contents differed significantly [18]. Further, finger citron leaf essential oil exhibits bioactivities, such as inhibiting bacterial proliferation and tumor cell viability [7,19]. These findings indicate that finger citron leaves complement fruit-based aroma research and have an independent research and development value. Recently, molecular docking technology has been increasingly applied to investigate the interactions between aroma compounds and olfactory receptors, offering a novel perspective for understanding aroma characteristics at the molecular level [20–23].

Against this background, the present study aimed to identify the volatile components of leaves from finger citron cultivars using HS-SPME-GC-MS, screen differential characteristic compounds among cultivars through multivariate statistical analysis, and determine the binding modes of key aroma-active compounds to olfactory receptors via molecular docking. The findings provide scientific evidence for the evaluation of germplasm resources, utilization of leaf by-products, and targeted regulation of aroma quality in finger citron.

2. Materials and Methods

2.1. Plant Materials and Equipment

Since harvesting young finger citron leaves affects plant growth, mature leaves were selected for the experiments. Finger citron leaves were collected on 2 May 2025, from the Jinhua Finger Citron Germplasm Repository in Jinhua City, Zhejiang Province, China. All of the cultivars had been cultivated at this base for more than two years, showed a uniform tree age of three years and consistent growth conditions, and were grown in the same controlled greenhouse facility. No pesticides were applied for 15 days prior to sampling. The following cultivars were tested (Figure 1): QingyiTongzi (QYTZ), Xiuzhen (XZ), Tianci (TC), Cuiyu (CY), Yangguang (YG), Kaixin (KX), Guangfoshou (GFS), and Yunfoshou (YFS). GFS and YFS seedlings were sourced from Lecheng Town, Gaoyao District, Zhaoqing City, Guangdong Province, and Tuantian Town, Mojiang County, Pu'er City, Yunnan Province, respectively. Six plants were randomly selected from each cultivar as biological replicates. Two fully mature leaves of similar size were collected from the spring shoots of each plant. The samples were ground in liquid nitrogen and evenly divided into three portions as technical replicates for the experiments.

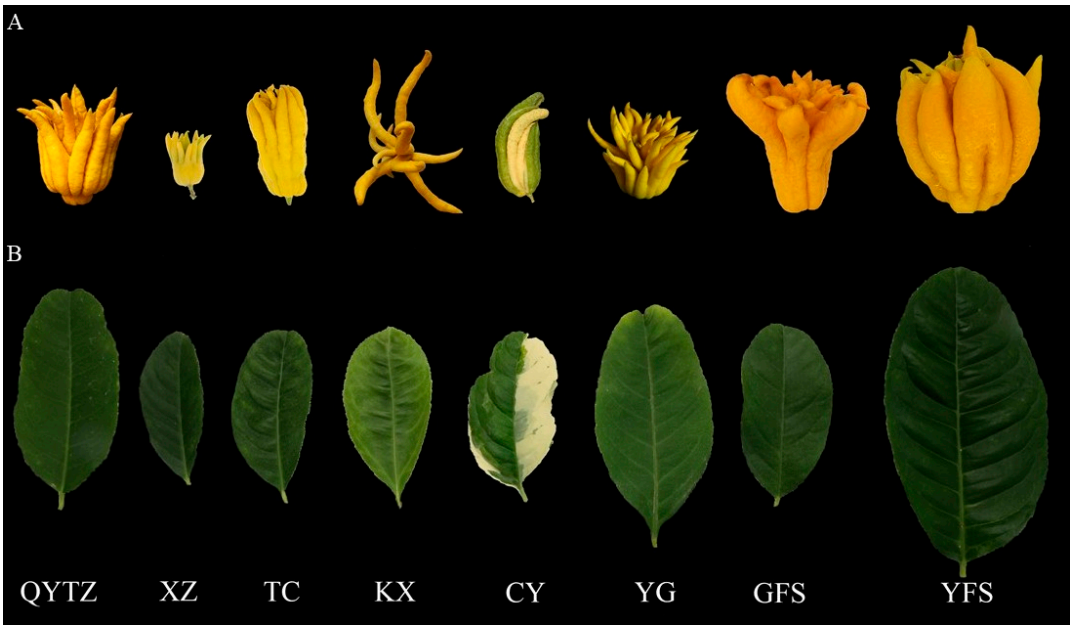


Figure 1. Photographs of fruit (**A**) and leaves (**B**) of eight finger citron cultivars. From left to right: QingyiTongzi (QYTZ), Xiuzhen (XZ), Tianci (TC), Cuiyu (CY), Yangguang (YG), Kaixin (KX), Guangfoshou (GFS), and Yunfoshou (YFS). The images are presented solely for representative morphological comparison.

The following instruments and equipment were used: 7000D triple quadrupole gas chromatography–mass spectrometry system (Agilent Technologies, Santa Clara, CA, USA); HP-5MS capillary column (30 m × 0.25 mm × 0.25 μm, Supelco, Bellefonte, PA, USA); 30/50 CAR/DVB/PDMS fiber assembly (Supelco, Bellefonte, PA, USA); and a constant-temperature water bath (JingHong Instrument Co., Ltd., Shanghai, China).

2.2. Headspace Solid-Phase Microextraction (HS-SPME)

The SPME fiber was preconditioned at 250 °C for 30 min prior to use to ensure fiber reliability [14]. A 500 mg aliquot of each sample was placed into a 20 mL headspace vial, and 2 mL of saturated NaCl solution and 20 μL of o-dichlorobenzene internal standard solution (10 μg/mL) were added. The vial was incubated in a constant-temperature water

bath at 60 °C for 30 min for adsorption. After incubation, the fiber was inserted into the GC injection port and thermally desorbed at 250 °C for 5 min.

2.3. GC-MS Conditions

For gas chromatography, separation was performed on an HP-5MS capillary column (30 m × 0.25 mm × 0.25 μm, Agilent Technologies, Santa Clara, CA, USA). The injector temperature was set at 250 °C, with helium as the carrier gas at a constant flow rate of 1.0 mL/min. Injection was conducted in splitless mode, and the solvent delay was set to 5 min. The oven temperature program was run as follows: initial temperature of 40 °C held for 3 min, ramped to 100 °C at 3 °C/min, and then ramped to 230 °C at 5 °C/min and held for 20 min.

The mass spectrometry conditions were as follows: electron ionization (EI) source at 70 eV; ion source temperature, 230 °C; interface temperature, 250 °C; only full-scan mode with a mass acquisition range of m/z 20–350.

2.4. Qualitative and Quantitative Analysis of Volatile Compounds

For qualitative analysis, retention indices (RIs) of the detected compounds were determined using a series of n-alkane standards (C_8–C_{30}). Compounds were identified by matching the mass spectra against the NIST 20.L Libraries, and only compounds with a matching degree greater than 80% were retained. The calculated RI of each compound was matched against the literature for qualitative confirmation, and a deviation of ±10 was allowed between the measured and literature RI values. For compounds whose RIs could not be calculated, those present in all three technical replicates were retained. The RI for each compound was calculated using the following formula:

$$RI = 100 \times n + 100 \times (t_a - t_n)/(t_{n+1} - t_n) \quad (1)$$

where t_a is the retention time of analyte peak a, and t_n and t_{n+1} are the retention times of the n-alkanes with carbon numbers n and n + 1, respectively.

For semi-quantitative analysis, the contents of volatile compounds were calculated using the internal standard method using the following formula:

$$C_a = (C_i \times V_i/M_0) \times (A_a/A_i) \quad (2)$$

where C_a is the volatile compound content (μg/g); C_i is the internal standard concentration (μg/g); V_i is the internal standard volume (mL); M_0 is the sample mass (g); A_a is the peak area of the volatile compound; and A_i is the peak area of the internal standard.

2.5. Relative Odor Activity Value (ROAV) Analysis

The contribution of each volatile compound to the overall aroma was evaluated using the relative odor activity value (ROAV) method, as described by Liu et al. [24], using the following formula:

$$ROAV_a = (C\%_a/C\%_{max}) \times (T_{max}/T_a) \times 100 \quad (3)$$

where $C\%_a$ is the relative volatile compound content, T_a is the odor threshold of the volatile compound (μg/g), and $C\%_{max}$ and T_{max} are the relative content and odor threshold, respectively, of the volatile compound contributing the most to the overall aroma of the sample.

The relative volatile compound contents were calculated based on mean values.

2.6. Molecular Docking

The three-dimensional (3D) structures of the 13 key aroma compounds were obtained from the PubChem database. The 3D structure model of human olfactory receptor family 1 subfamily A member 1 (OR1A1) was downloaded from the UniProt database (UniProt ID: Q9P1Q5). As an experimentally determined crystal or cryo-electron microscopy (cryo-EM) structure is not currently available for OR1A1, its 3D structure model was determined from the AlphaFold DB predicted structure (AlphaFoldDB: AF-Q9P1Q5-F1). Water molecules and the original ligand were removed using PyMOL 3.0.3. The receptor protein was processed using AutoDock Tools 1.5.7, and the receptor and ligands were saved in PDBQT format. Potential binding pockets on OR1A1 were predicted using Cyscore (http://clab.labshare.cn/software/cyscore.html, accessed 10 Apr 2026), generating five candidate binding sites [25]. Semi-flexible molecular docking was performed using AutoDock Vina 1.2.7, with nine binding conformations independently generated for each candidate pocket [26]. The five pockets with the lowest binding energies were compared, and the pocket with the highest absolute binding energy was selected as the most probable ligand-binding site. The predicted key interacting residues were compared to those reported in site-directed mutagenesis studies, including Tyr251, Tyr258, and Phe206, to validate the docking protocol [27–30]. When the predicted residues were consistent with the experimentally validated residues mentioned above, the validity of the docking results was supported. The conformation corresponding to the lowest binding energy was visualized using PyMOL 3.0.3.

2.7. Data Statistics and Analysis

Each technical replicate was treated as a single sample for data analysis. Compounds were classified based on the in-house database of Wuhan Metware Biotechnology Co., Ltd. (Wuhan, Hubei, China). R software (version 4.4.3) was used to perform principal component analysis (PCA), orthogonal partial least squares discriminant analysis (OPLS-DA), and cluster heatmap analysis. The *p*-values used for differential compound screening were calculated using a Student's *t*-test and adjusted for multiple comparisons using the Benjamini–Hochberg false discovery rate correction.

3. Results

3.1. Analysis of Volatile Compound Categories in Leaves of Finger Citron Cultivars

In this study, retention indices and mass spectral match factors were used as the sole criteria for VOC identification. Accordingly, compound assignments should be regarded as tentative, and the corresponding results serve only as semi-quantitative references. A total of 394 volatile compounds were tentatively detected in the leaves of the 8 finger citron cultivars (Figure 2), which were classified into 14 chemical categories as follows: 34 aldehydes, 94 terpenoids, 67 alcohols, 19 ketones, 27 aromatic hydrocarbons, 81 esters, 4 phenols, 3 amines, 31 hydrocarbons, 13 acids, 5 ethers, 2 amides, 5 nitrogen-containing compounds, and 9 heterocyclic compounds. Terpenoids constituted the highest proportion in all of the cultivars except YG, with the highest percentage (43.43%) observed in XZ. Esters had the highest relative content in YG. Ethers were only detected in TC, KX, YG, and YFS, and amides were detected only in QYTZ, TC, GFS, and YFS. Phenols were not detected in QYTZ, CY, or GFS.

3.2. Comparison of Volatile Compound Contents in Leaves of Finger Citron Cultivars

Semi-quantitative results showed that YFS had the highest relative content of total volatiles, while the other cultivars were generally lower (Figure 3D). As shown in Figure 3B, neral had the highest relative content in QYTZ, followed by geranial. (+)-Sylvestrene was

the most abundant compound in XZ, YG, and YFS, whereas geranial predominated in TC, KX, CY, and GFS. Analysis of the volatile profiles among the eight cultivars revealed that YG had 46 unique volatile components, including cis-calamenene, nerolidol, and 1-hexadecanol (Figure 3C; Supplementary Table S1). There were 37 unique volatile components, including phenol, 2-methoxy-, trans-rose oxide, and α-maaliene, in YFS. TC, GFS, KX, QYTZ, CY, and XZ contained 18, 17, 16, 14, 12, and 2 unique components, respectively. A total of 23 volatile compounds were common among all eight of the cultivars.

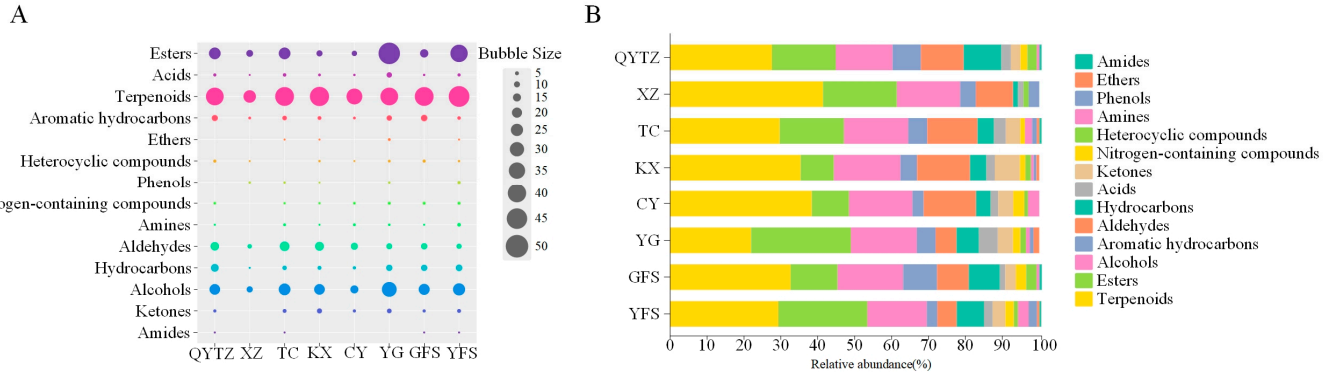


Figure 2. Comparison of volatile compound categories in leaves of finger citron cultivars: (**A**) bubble plot showing the number of volatile compounds in each category across cultivars; (**B**) relative contents of volatile compound classes in leaves of finger citron cultivars (calculated based on the relative concentrations of compounds).

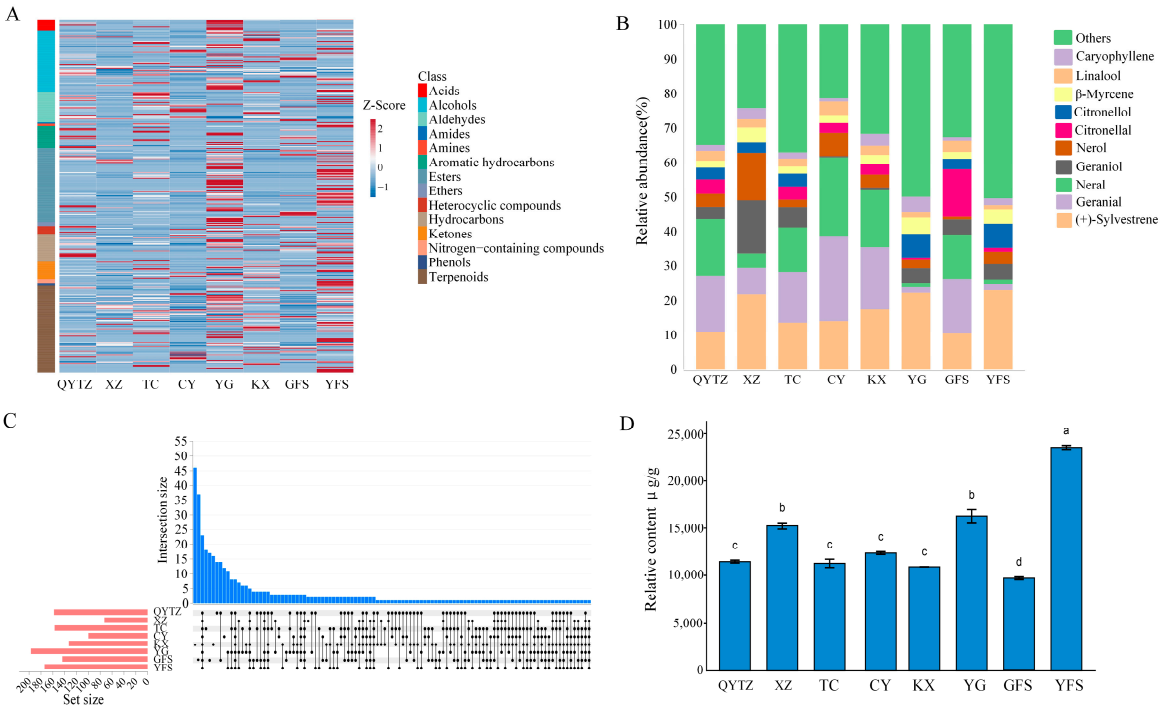


Figure 3. Comparison of volatile compound contents in leaves of finger citron cultivars: (**A**) heatmap of volatile compound contents, with data normalized using Z-score across the compound dimension; (**B**) proportional distribution of the top 10 compounds with the highest relative contents; (**C**) upset plot showing the unique and shared volatile compounds among the eight finger citron cultivars; (**D**) total volatile content of each cultivar. Different lowercase letters above the bars indicate statistically significant differences among cultivars ($p < 0.05$).

3.3. Analysis of Differential Volatile Compounds Among Finger Citron Cultivars

PCA and OPLS-DA were used to explore differences in the volatile composition of pooled leaf samples from different cultivars. PCA showed that the three technical replicates of each cultivar grouped together (Figure 4A), indicating good consistency among replicates. The variance contribution rates of PC1 and PC2 were 42.85 and 17.41%, respectively, with a cumulative variance contribution rate of 60.26%. QYTZ, XZ, TC, CY, KX, and GFS clustered together, suggesting that these cultivars shared similar volatile compositions. YG and YFS each formed separate clusters positioned at a distance from the others, indicating differences in leaf volatile profiles compared to the remaining cultivars.

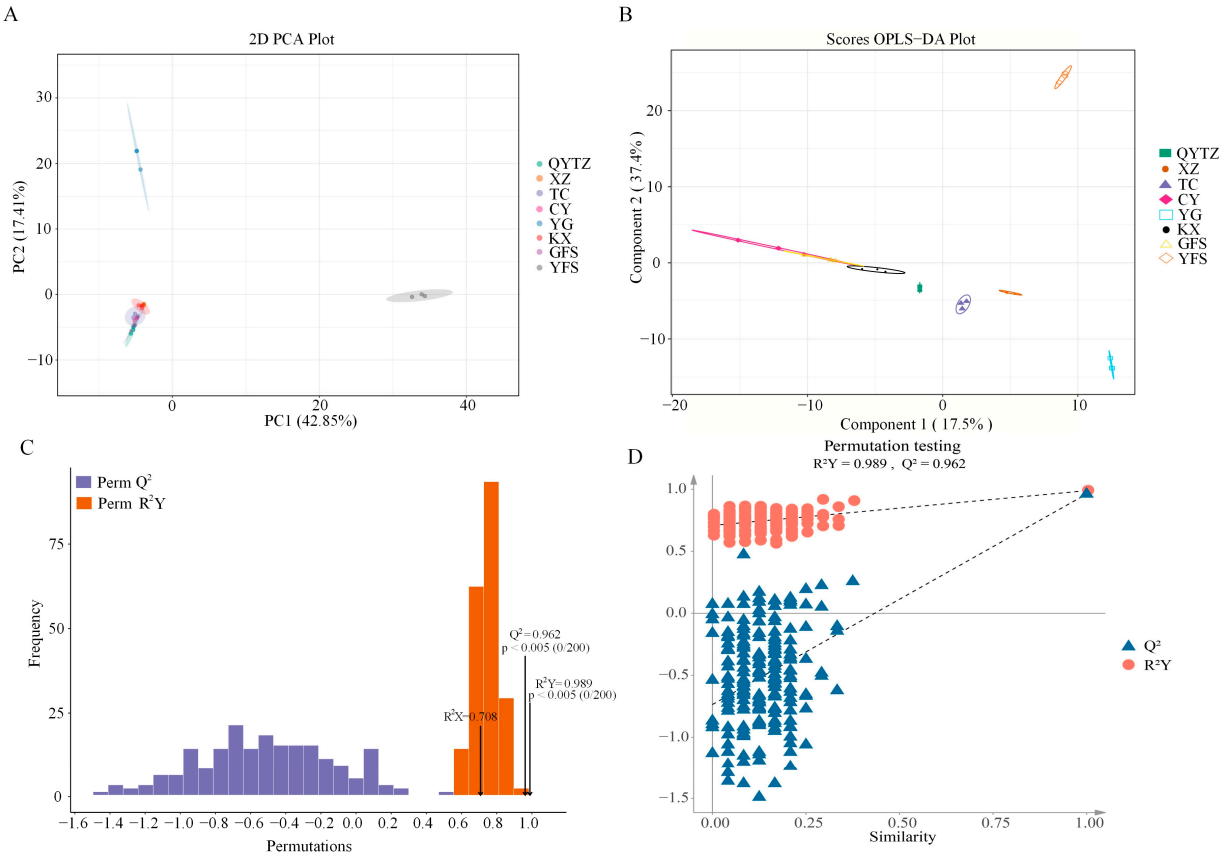


Figure 4. PCA and OPLS-DA of volatile compounds in leaves of finger citron cultivars: (**A**) PCA score plot; (**B**) OPLS-DA score plot; (**C**) validation plot; (**D**) OPLS-DA permutation test plot (based on 200 permutations).

The OPLS-DA model (Figure 4C) showed the following parameters: R^2X = 0.708, R^2Y = 0.989, and Q^2 = 0.962. Based on the results of 200 permutation tests (Figure 4D), the intercept of the Q^2 regression line was < 0, and Q^2 = 0.962, indicating that the model is reliable and free from overfitting. However, this model was still based on technical replicates and therefore constitutes an exploratory analysis. OPLS-DA (Figure 4B) revealed that YFS and YG were distantly separated from the other cultivars, consistent with the PCA findings. Based on the criteria of VIP > 1 and $p < 0.05$, potential discriminant compounds for each cultivar relative to the others were preliminarily screened, with 88, 95, 92, 85, 106, 87, 87, and 134 compounds identified in QYTZ, XZ, TC, CY, YG, KX, GFS, and YFS, respectively (Figure 5). These compounds show potential for discriminating among finger citron leaves of different cultivars; however, the observed differences remain to be further validated with independent biological replicates.

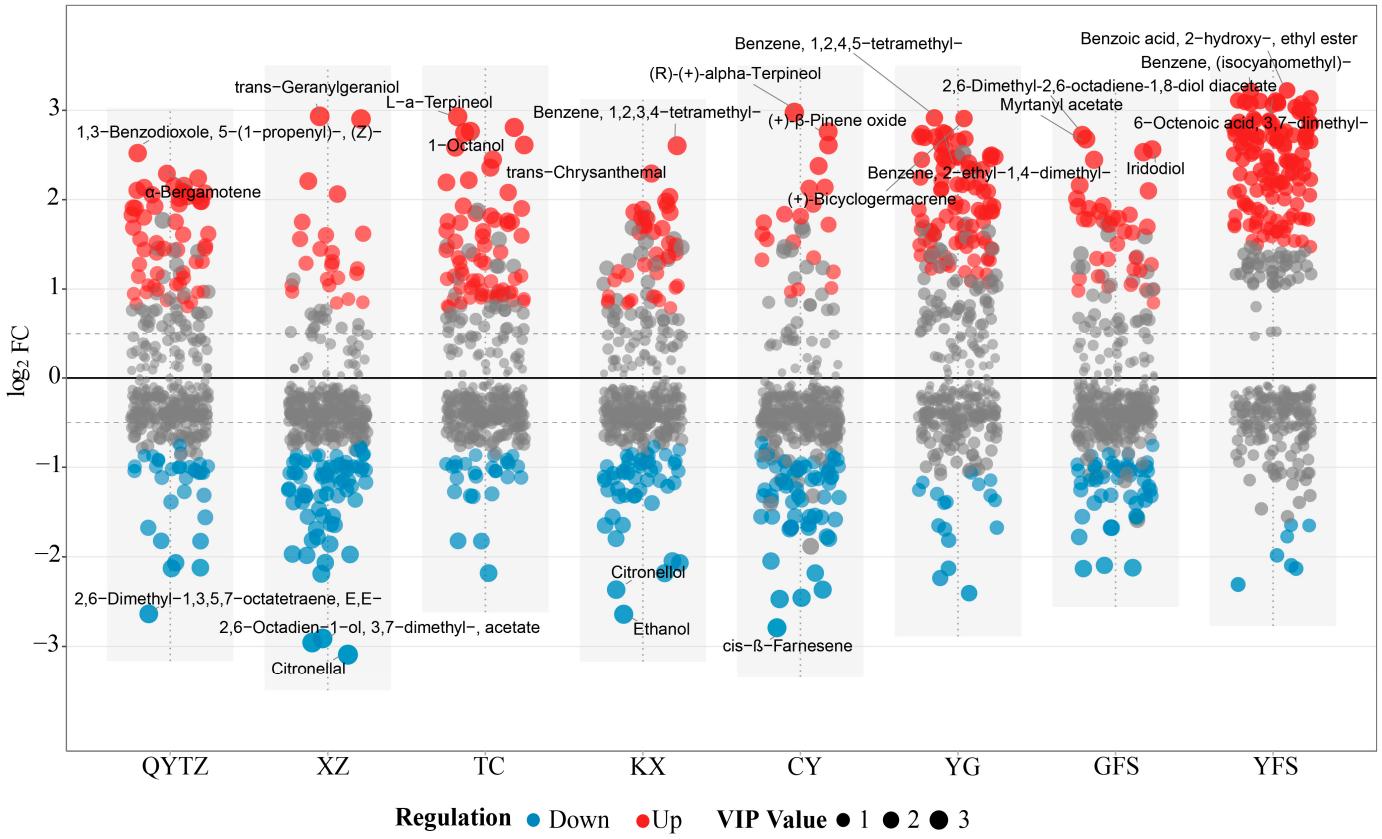


Figure 5. Multi-group comparison of differential volatile compounds in leaves of finger citron cultivars. Red and blue dots represent upregulated and downregulated volatile compounds, respectively, whereas grey dots represent compounds that did not meet the differential criteria.

3.4. Analysis of Key Aroma Compounds in Leaves of Finger Citron Cultivars

Theoretically, ROAVs calculated using air thresholds most closely reflect the actual perception of leaf aroma. However, determining air thresholds is influenced by various factors, including the detection method and subject population, and the values reported for the same compound vary widely among studies. Therefore, water thresholds, which are based on a more mature database and show lower variability, were selected for the calculation. As shown in Table 1, a total of 13 volatile compounds exhibited an ROAV greater than 1 across all of the cultivars, with variations in the number and type of key aroma components among cultivars. Specifically, QYTZ, XZ, TC, CY, YG, KX, GFS, and YFS contained 7, 6, 8, 4, 6, 7, 6, and 10 key compounds, respectively. Linalool consistently exhibited the highest ROAV value across cultivars, contributing the floral note to finger citron leaves. In addition to linalool, geraniol and β-myrcene in QYTZ contributed floral, fruity, and herbal notes. In XZ, linalool and geraniol had relatively high ROAVs, resulting in an overall floral and fruity profile. In addition to linalool, geraniol and β-myrcene contributed floral–fruity and herbal notes to TC. Among all of the cultivars, the ROAV of linalool was lowest in YG, whereas that of β-myrcene was highest. CY exhibited the simplest aroma profile, characterized by floral notes. Linalool, β-myrcene, and geraniol showed relatively high estimated aroma contributions to YG. Linalool, β-myrcene, geraniol, and nonanal had relatively high ROAVs in KX, imparting floral, fruity, and orange peel-like notes. Linalool, geraniol, and β-myrcene had relatively high ROAVs in GFS, resulting in an overall floral and dry woody profile. Linalool, geraniol, β-myrcene, and nonanal showed relatively high ROAVs in YFS, contributing floral, sweet fruity, herbal, and woody notes.

Table 1. ROAV analysis of volatile compounds in leaves of finger citron cultivars.

Components	CAS	Aromatic Thresholds (μg/g)	QYTZ	XZ	TC	CY	YG	KX	GFS	YFS	Aroma Characteristic
Linalool	78-70-6	0.00022	38.15	38.69	36.32	40.58	35.83	36.96	37.71	52.08	floral
Geraniol	106-24-1	0.0011	7.95	10.18	8.53	4.94	8.54	5.91	7.93	12.13	floral, fruity
Naphthalene	91-20-3	0.006	1.17	0.00	0.00	0.00	0.29	0.35	1.06	0.00	dry
Styrene	100-42-5	0.0036	1.83	2.06	1.79	1.95	2.02	1.96	1.86	3.03	sweet
Decanal	112-31-2	0.003	1.51	1.17	2.37	0.00	0.88	2.44	1.67	2.96	orange peel
Nonanal	124-19-6	0.0011	0.00	0.00	5.92	0.00	0.00	4.27	0.00	7.64	orange peel
Phenylacetaldehyde	122-78-1	0.0063	0.27	0.00	0.24	0.24	0.00	0.14	0.00	1.13	citrus, fruity
Germacrene D	23986-74-5	0.0012 [31]	1.30	0.00	0.00	0.00	0.00	1.39	0.00	0.00	woody
β-Myrcene	123-35-3	0.0012	6.53	7.84	6.51	6.82	7.97	6.84	6.29	11.10	balsam, herbal
α-Ionone	127-41-3	0.00378	0.00	0.00	0.00	0.00	0.00	0.00	0.00	1.19	floral, woody
δ-Cadinene	483-76-1	0.0015	0.00	1.83	2.88	0.67	3.28	0.00	0.00	4.62	herbal, woody
Ethyl caprate	110-38-3	0.005	0.98	0.32	1.05	0.00	1.04	0.00	0.00	0.00	fruity
Ethyl cinnamate	4192-77-2	0.0007 [32]	0.00	0.00	0.00	0.00	0.00	0.00	0.00	12.31	floral

Note: Thresholds for compounds not specifically annotated were sourced from Compilations of Odour Threshold Values in Air, Water and Other Media [33]. Aroma characteristics were obtained from the following website: http://www.thegoodscentscompany.com.

3.5. Molecular Docking of Key Aroma Compounds with the Human Olfactory Receptor OR1A1

OR1A1 is a human olfactory receptor protein that is primarily expressed in the olfactory epithelial cells of the nasal cavity, where it plays a critical role in olfactory perception [30]. Molecular docking was performed to analyze the interactions among the 13 volatile compounds with an ROAV > 1 and the human olfactory receptor OR1A1 (Table 2 and Figure 6). The binding energies of the 13 volatile compounds ranged from −5.859 to −8.652 kcal/mol, suggesting that these compounds interact favorably with the predicted OR1A1 binding site. Among the 13 compounds, decanal, ethyl caprate, geraniol, nonanal, and phenylacetaldehyde formed hydrogen bonds with OR1A1, whereas the remaining eight compounds did not form hydrogen bonds but instead interacted with the amino acid residues of OR1A1 primarily through hydrophobic interactions. The amino acid residue Asn109 formed hydrogen bonds with decanal, ethyl caprate, geraniol, nonanal, and phenylacetaldehyde. Except for ethyl cinnamate and naphthalene, the key aroma compounds exhibited hydrophobic interactions with the Tyr258 residue.

Table 2. Molecular docking of 13 volatile compounds with olfactory receptor OR1A1.

Ligand	Binding Energy (kcal/mol)	Hydrogen Bond Residue	Hydrophobic Interaction Residue
α-Ionone	−7.832	-	Tyr258, Phe206, Val203, Val254, Ile105, Ile181
Decanal	−5.859	Asn109, Asn155	Val254, Tyr276, Phe206, Phe73, Tyr258
δ-Cadinene	−8.652	-	Phe206, Tyr258, Val203, Val254, His159, Ile181, Ile105
Ethyl caprate	−6.524	Asn155, Asn109	Phe73, Tyr276, Met104, Tyr258, Val254, Phe206, Ile105, His159
Ethyl cinnamate	−7.452	-	Val203, Phe206, Tyr276, Phe73, Met104
Geraniol	−6.597	Gly202, Asn109	Tyr258, Val203, Phe206, Val254, Tyr276, Met104, Ile105, Tyr178
Germacrene D	−7.72	-	Phe206, Met104, Ile105, Ile181, His159, Tyr258
Linalool	−6.413	-	Val254, Phe206, Val203, Tyr258, Ile105, His159, Ile181
Myrcene	−6.314	-	Phe206, Val203, Ile105, Ile181, His159, Met199, Tyr258, Val254
Naphthalene	−7.498	-	Val203, Phe206, Val254
Nonanal	−5.628	Asn155, Asn109	Val254, Tyr276, Tyr258, Phe206
Phenylacetaldehyde	−6.102	Asn109, Met104	Tyr258, Val203
Styrene	−5.989	-	Tyr258, Val254, Tyr276

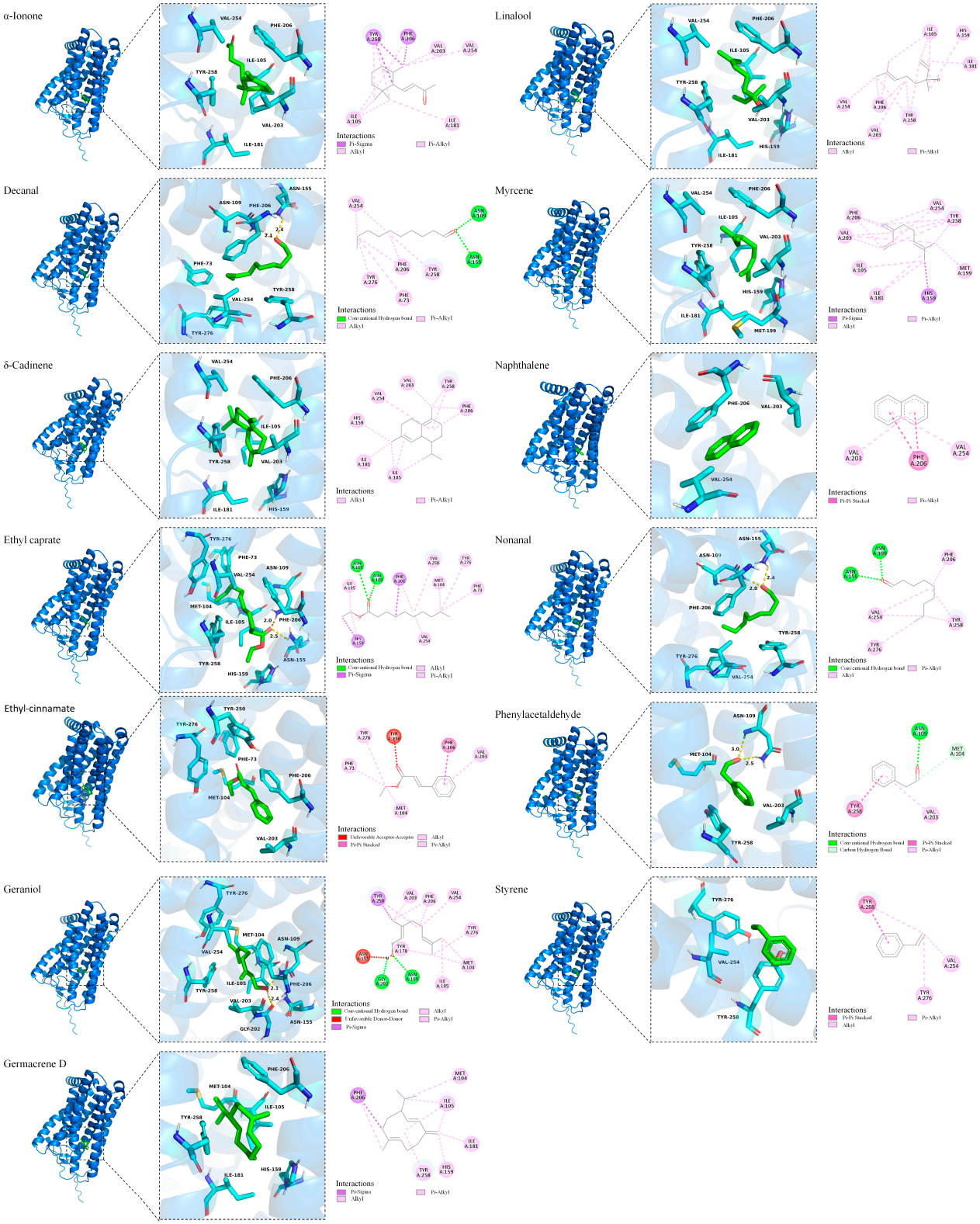


Figure 6. Predicted binding modes of 13 key aroma compounds with human olfactory receptor OR1A1. For each compound, the three-dimensional binding conformation is presented on the left, and the corresponding two-dimensional interaction diagram is shown on the right. In the 2D diagrams, hydrogen bonds are represented by green dashed lines, hydrophobic interactions by pink and purple dashed lines, and unfavorable donor–donor bonds by red dashed lines.

4. Discussion

Current research on volatile compounds in *Citrus* plants has predominantly focused on fruit, with limited attention given to leaves. In this study, HS-SPME-GC-MS was used to detect volatile compounds in the leaves of eight finger citron cultivars cultivated under identical environmental conditions and in trees of a similar age. A total of 394 volatile compounds were tentatively identified, minimizing the influence of environmental factors on the volatile compounds as much as possible. However, in this study, only one pooled biological sample and three technical replicates were available for each cultivar. In addition, compound identification relied mainly on mass spectral library matching and RI comparison, without validation against authentic reference standards. Therefore, the results should be considered preliminary and semi-quantitative. In a previous study, only 40 volatile compounds were detected in the mature leaves of cultivar QYTZ [34], which may be attributed to differences in the cultivation environment, detection method, or sampling time. This study detected dimethylamine, dimethyl phthalate, nitrosomethane, and other compounds that appeared anomalous as naturally occurring volatiles in *Citrus* leaves. We speculate that these compounds may originate from agrochemicals, mineral oils, natural small-molecule compounds, and other sources affecting cultivation. However, current evidence is insufficient to confirm whether they are of endogenous plant origin. In future studies, pesticide application during cultivation should be controlled to clarify the volatile compounds in finger citron leaves. Terpenoids constituted the most abundant chemical class in QYTZ, XZ, TC, KX, CY, GFS, and YFS, a finding consistent with that in other *Citrus* species [35–38]. Although esters were the most abundant category in YG, the top 10 compounds in terms of relative content belonged to terpenoids, accounting for 50.1% of the total. This discrepancy may result from differences in compound classification criteria.

In the present study, neral was the most abundant compound in QYTZ leaves, followed by geranial, and limonene was detected at only 22.80 μg/g. However, Xu et al. reported that limonene was the most abundant compound in mature leaves of QYTZ, followed by geranial [34]. Azam et al. found that young leaves produced more volatile compounds than mature leaves in most *Citrus* cultivars and that the aldehyde content increased during leaf development [39]. Therefore, differences in leaf age may account for the higher neral and geranial contents observed in QYTZ in this study. Notably, (+)-sylvestrene exhibited a relatively high content in all of the evaluated cultivars and was even the most abundant volatile compound in XZ, YG, and YFS. Although (+)-sylvestrene has been detected in *Citrus* plants in previous studies, its content was generally low [40–42]. Prior studies have demonstrated that (+)-sylvestrene biosynthesis in plants is significantly upregulated in response to herbivore attack [43]. Given that all of the leaves collected in this study were obtained from greenhouse cultivation with frequent mite infestation, we speculate that mite damage to the sampled leaves contributed to the relatively high (+)-sylvestrene content. Future studies should collect finger citron leaves exposed to varying degrees of mite infestation to elucidate the role of (+)-sylvestrene in plant defense.

Analysis of differential volatile compounds among the finger citron cultivars preliminarily indicated that QYTZ, XZ, TC, CY, KX, and GFS had relatively similar volatile compositions. The first five of these cultivars were derived from bud mutation breeding in Jinhua, Zhejiang Province, and their similar genetic backgrounds likely contributed to the observed compositional similarity. The clustering of GFS with these cultivars suggests that its aroma composition was relatively similar to theirs; however, given that only one pooled biological sample and three technical replicates were used per cultivar in this study, no conclusion can be drawn regarding whether significant differences exist among these cultivars. YG, which was introduced from Yunnan Province and has undergone long-term domestication/acclimatization in Zhejiang, displayed a relatively distinct volatile profile in

the present pooled-sample analysis, suggesting that genes involved in volatile biosynthesis may have been altered during domestication/acclimatization; however, this inference remains preliminary and requires validation with independent biological replicates.

As an ornamental potted plant, finger citron quality is partly determined by the aroma components of its leaves. In this study, YFS had the highest total volatile content, suggesting its potential for high-quality potted plant production and as a raw material for aroma enhancement-oriented breeding. Nevertheless, whether YFS is the best choice for essential oil extraction requires further investigation into extraction methods, yields, and extract composition.

In this study, the ROAVs of volatile compounds from eight finger citron cultivars were analyzed. Linalool, geraniol, naphthalene, styrene, decanal, nonanal, phenylacetaldehyde, germacrene D, β-myrcene, α-ionone, δ-cadinene, ethyl caprate, and ethyl cinnamate were identified as contributing most to finger citron leaf aroma. Linalool is a widely distributed volatile compound in citrus plants and has been recognized as a key aroma-active compound in citrus fruit, flowers, and leaves [44–47]. Geraniol, styrene, and β-myrcene exhibited an ROAV greater than 1 in all of the finger citron leaf samples, indicating their ubiquitous contributions to the aroma profiles of all of the cultivars. Geraniol imparts floral notes, styrene contributes sweet notes, and β-myrcene conveys balsamic and herbal nuances. However, finger citron leaves are a complex plant matrix containing essential oils, lipid-soluble pigments, and a waxy layer, and the microenvironment for aroma release is between the aqueous and oil phases. Ronald found that the logarithmic reciprocal ratio of thresholds showed a significant linear relationship with the octanol/water partition coefficient of compounds, suggesting that the more lipophilic a compound, the greater the difference between its threshold in water and that in oil [48]. A study on tomato aroma has shown that the perception of volatile compounds undergoes qualitative and quantitative changes in different media and that ethanol and methanol alter the perception of tomato aroma [49]. Therefore, the results calculated based on aqueous thresholds in this study may overestimate the contribution of lipophilic terpenoids, such as β-myrcene, linalool, and δ-cadinene, to the aroma of finger citron leaves. The difference between the actual perception thresholds of hydrophilic compounds, such as phenylacetaldehyde, in water and in the leaf matrix is smaller than that of lipophilic compounds, leading to an underestimation of hydrophilic compounds' contribution to aroma. In future studies, gas chromatography–olfactometry can be used to perform sensory validation of the screened compounds, which may, to some extent, compensate for the uncertainty caused by the mismatch between threshold media.

Molecular docking showed that δ-cadinene had the lowest predicted binding energy with OR1A1, indicating a relatively strong binding tendency. Linalool, which had the highest ROAV, did not form hydrogen bonds with OR1A1 in the docked conformation, but its hydrophobic skeleton interacted with residues such as Tyr258, Val254, and Phe206 through hydrophobic interactions, potentially contributing to its complex stability, consistent with trends reported in previous studies [50–52]. In the docking model, the primary hydroxyl group of geraniol formed hydrogen bonds with Asn109 and Gly202, whereas no hydrogen bonds were observed for styrene or β-myrcene in their docked conformations, and their binding appeared to be mainly driven by hydrophobic interactions. These results are predictions based on molecular docking and require further validation through experiments or molecular dynamics simulations. This study primarily explored the aroma perception mechanism from the perspective of molecular docking between individual compounds and olfactory receptor OR1A1, but interactions among aroma compounds can also influence olfactory perception. Studies have shown that linalool and α-ionone have synergistic effects, enhancing the perception of floral notes [53,54]. Linalool and β-myrcene can lower

each other's olfactory thresholds when mixed [55], and geraniol and nonanal produce perceptual fusion [56]. Therefore, future research should investigate the aroma profiles of finger citron leaves through sensory evaluation and aroma recombination experiments.

5. Conclusions

Compared to finger citron fruit, finger citron leaves are more readily available and represent an ideal raw material for essential oil extraction. In this study, based on pooled samples of six individual plants per cultivar, HS-SPME-GC-MS was used to analyze the volatile compounds in leaves of finger citron cultivars, tentatively identifying 394 compounds, among which terpenoids constituted the highest proportion. In this pooled-sample analysis, preliminary differences in volatile composition were observed among cultivars, with (+)-sylvestrene, geranial, and neral being the three most abundant compounds. YFS had the relatively highest total volatile content, making it a promising candidate as a raw material for essential oil production that warrants further evaluation. The volatile compositions of QYTZ, XZ, TC, CY, KX, and GFS were relatively similar to one another but differed relatively greatly from those of YG and YFS. Among all of the cultivars, linalool exhibited the highest ROAV. In terms of aroma characteristics, QYTZ, XZ, TC, KX, YG, and GFS were predominantly characterized by floral and herbal notes that were supplemented with fruity and woody notes. CY had a relatively simple aroma profile dominated by floral notes, and YFS presented a complex aroma profile integrating floral, sweet fruity, herbal, and woody notes. The molecular docking binding energies of the 13 key aroma compounds with human olfactory receptor OR1A1 ranged from −5.859 to −8.652 kcal/mol, suggesting that these compounds interact favorably with the predicted OR1A1 binding site. The molecular docking model predicted that Asn109 and Tyr258 are involved in hydrogen bonding and hydrophobic interactions, respectively. Future studies should analyze the aroma composition of leaves at different developmental stages, in combination with independent biological replicates, to determine the optimal harvest period. Furthermore, aroma recombination and omission experiments should be performed to validate the actual sensory contributions of the key aroma compounds identified herein, and site-directed mutagenesis and functional assays of OR1A1 are warranted to further confirm the predicted binding mechanisms.

Supplementary Materials: The following supporting information can be downloaded at https://www.mdpi.com/article/10.3390/horticulturae12101289/s1, Table S1: Volatile compounds tentatively identified in leaves of different finger citron cultivars (μg/g).

Author Contributions: Resources, Y.W. and J.S.; writing—original draft preparation, J.W., Y.Z. and B.L.; writing—review and editing, J.W., Y.Z. and X.L.; visualization, J.W., Y.Z. and Y.C.; supervision, C.C.; project administration, P.S. and Y.W.; funding acquisition, Y.W. and J.S. All authors have read and agreed to the published version of the manuscript.

Funding: This research was funded by Identification, Evaluation, and Utilization of Characteristic Aroma Components in Jinhua Finger Citron Resources (2023-2-003) and Jindong District Fruit and Flower Industry Team Science and Technology Commissioner Project.

Data Availability Statement: The original contributions presented in this study are included in the article/Supplementary Materials; further inquiries can be directed to the corresponding authors.

Conflicts of Interest: The authors declare that they do not have any conflicts of interest.

References

1. Luo, X.; Wang, J.; Chen, H.; Zhou, A.; Song, M.; Zhong, Q.; Chen, H.; Cao, Y. Identification of Flavoanoids From Finger Citron and Evaluation on Their Antioxidative and Antiaging Activities. *Front. Nutr.* **2020**, *7*, 584900. [CrossRef] [PubMed]
2. Ma, J.-J.; Xie, X.; Ma, L.-K.; Wang, Q.; Xiao, G.-S.; Liu, H.-F. Structural characterization and hypolipidemic activity of polysaccharides from finger citron. *J. Funct. Foods* **2026**, *138*, 107185. [CrossRef]

3. Yang, K.-M.; Chen, H.-C.; Chuang, C.-H.; Chiang, Y.-C.; Lin, L.-Y. Effects of Fingered Citron (*Citrus medica* var. sarcodactylis) Essential Oil on Improvement in Diet-Induced Hyperlipidemia Syrian Hamsters. *J. Oleo Sci.* **2025**, *74*, 321–328. [CrossRef] [PubMed]
4. Chen, J.; Shi, J.; Gu, W.; Li, W.; Lyu, R.; Wu, X.; Wang, J.; Liu, C. Multi-Target Antidepressant Action of *Citrus medica* L. var. sarcodactylis Swingle (Bergamot) Essential Oil: From PI3K/AKT-Driven Apoptosis Inhibition to BDNF/5-HT Signaling Activation. *S. Afr. J. Bot.* **2025**, *185*, 422–436. [CrossRef]
5. Fratianni, F.; Cozzolino, A.; De Feo, V.; Coppola, R.; Ombra, M.N.; Nazzaro, F. Polyphenols, Antioxidant, Antibacterial, and Biofilm Inhibitory Activities of Peel and Pulp of *Citrus medica* L., *Citrus bergamia*, and *Citrus medica* cv. Salò Cultivated in Southern Italy. *Molecules* **2019**, *24*, 4577. [CrossRef] [PubMed]
6. Li, Z.-H.; Cai, M.; Liu, Y.-S.; Sun, P.-L.; Luo, S.-L. Antibacterial Activity and Mechanisms of Essential Oil from *Citrus medica* L. var. sarcodactylis. *Molecules* **2019**, *24*, 1577. [CrossRef] [PubMed]
7. Luo, C.; Li, D.; Wang, Y.; Guo, S.; Zhang, D.; Du, S. Chemical Composition and Insecticide Efficacy of Essential Oils from *Citrus medica* L. var. sarcodactylis Swingle Against *Tribolium castaneum* Herbst in Stored Medicinal Materials. *J. Essent. Oil Bear. Plants* **2019**, *22*, 1182–1194. [CrossRef]
8. Cui, C.; Sun, L.; Huang, X.; Nie, Z.; Zhu, Y.; Wang, L.; Yang, Y.; Xing, X.; Ke, F. Integrated metabolomic and transcriptomic analyses reveal aroma diversity and its regulatory networks in aromatic acidic citrus. *Front. Plant Sci.* **2026**, *17*, 1785725. [CrossRef] [PubMed]
9. Ji, C.; Liu, C.; Wang, R.; Ruan, M.; Yao, Z.; Wan, H.; Li, Z.; Cheng, Y.; Ye, Q. The Science behind vegetable aromas: Types, synthesis, and influencing factors of volatile compounds. *Plant Signal. Behav.* **2025**, *20*, 2527958. [CrossRef] [PubMed]
10. Lu, H.; Zhao, H.; Zhong, T.; Chen, D.; Wu, Y.; Xie, Z. Molecular Regulatory Mechanisms Affecting Fruit Aroma. *Foods* **2024**, *13*, 1870. [CrossRef] [PubMed]
11. Goldenberg, L.; Yaniv, Y.; Doron-Faigenboim, A.; Carmi, N.; Porat, R. Diversity among mandarin varieties and natural sub-groups in aroma volatiles compositions. *J. Sci. Food Agric.* **2016**, *96*, 57–65. [CrossRef] [PubMed]
12. Yator, M.; Porat, R.; Masok, O.; Yaniv, Y.; Arad, T.; Goldenberg, L.; Carmi, N. Fruit quality, flavor and aroma volatiles compositions of the new superior mandarin varieties 'Einav', 'Saar', 'Sigal', 'Tamar', and 'Orit'. *Int. J. Food Prop.* **2025**, *28*, 2554888. [CrossRef]
13. Zhang, C.; Wang, C.; Wang, H.; Ablimit, A.; Sun, Q.; Dong, H.; Zhang, B.; Hu, W.; Liu, C.; Wang, C. Identification of characteristic volatiles and metabolomic pathways during the fermentation of red grapefruit by *Monascus purpureus* using HS-SPME-GC–MS and metabolomics. *Food Chem.* **2025**, *464*, 141786. [CrossRef] [PubMed]
14. Xu, Y.; Wang, Y.; Li, R.; Sun, P.; Chen, D.; Shen, J.; Feng, T. Characteristic aroma analysis of finger citron in four different regions based on GC–MS-HS-SPME and ROAV. *J. Food Process. Preserv.* **2022**, *46*, e17191. [CrossRef]
15. Song, S.; Tong, Y.; Feng, T.; Zhu, J. Multi-analysis of Odorous Compounds in Finger Citron (*Citrus medica* L. var. sarcodactylis Swingle) and Certification of Key Compounds. *J. Essent. Oil Bear. Plants* **2018**, *21*, 600–613. [CrossRef]
16. Wei, L.; Yu, X.; Li, H.; Zhu, M.; Pu, D.; Lu, Q.; Bao, Y.; Zu, Y. Optimization of solvent-free microwave extraction of essential oil from the fresh peel of *Citrus medica* L. var. arcodactylis Swingle by response surface methodology, chemical composition and activity characterization. *Sci. Hortic.* **2023**, *309*, 111663. [CrossRef]
17. Amézquita, E.J.; Quigley, M.Y.; Ophelders, T.; Seymour, D.; Munch, E.; Chitwood, D.H. The shape of aroma: Measuring and modeling citrus oil gland distribution. *Plants People Planet* **2023**, *5*, 698–711. [CrossRef]
18. Lin, H.; Zhu, M.; Jin, Z.; Yang, L.; Ren, H.; Yuan, M. Comparative Analysis of Volatile Oil Components of *Citrus medica* L. var. Sarcodactylis Swingle Fruit and Leaf by GC-MS. *Asia-Pac. Tradit. Med.* **2023**, *19*, 53–56.
19. Aliyah; Himawan, A.; Rante, H.; Mufidah; Ningsih, D.R. GC-MS analysis and antimicrobial activity determination of *Citrus medica* L. var proper leaf essential oil from South Sulawesi against skin pathogen microorganism. *IOP Conf. Ser. Mater. Sci. Eng.* **2017**, *259*, 012001. [CrossRef]
20. Jia, X.; Gao, Y.; Xi, H.; Cui, C.; Yang, X.; He, B.; Xu, C.; Gao, M.; Li, T. A flavor imitation method for *Osmanthus aroma* based on molecular docking screening and odor activity value analysis. *LWT* **2025**, *223*, 117697. [CrossRef]
21. Xiao, Z.; Gao, J.; Niu, Y.; Wang, Z.; Zhou, R.; Zhang, J.; Zhu, J. Elucidation of the sweetening mechanism of sweet orange fruit aroma compounds on sucrose solution using sensory evaluation, electronic tongue, molecular docking, and molecular dynamics simulation. *LWT* **2024**, *205*, 116555. [CrossRef]
22. Feng, S.; Gmitter, F.G., Jr.; Grosser, J.W.; Wang, Y. Identification of Key Flavor Compounds in Citrus Fruits: A Flavoromics Approach. *ACS Food Sci. Technol.* **2021**, *1*, 2076–2085. [CrossRef]
23. Xie, L.; Dong, Y.; Qin, Q.; Jiang, C.; Shang, L.; Qiao, K.; Wang, B.; Zeng, J.; Luo, Q.; Zhong, L.; et al. Integrated Flavoromics and Metabolomics Reveal Aroma and Bioactive Characteristics of Six Mainstream Citri Reticulatae Pericarpium Cultivars. *Foods* **2026**, *15*, 2090. [CrossRef] [PubMed]
24. Liu, D.-Y.; Zhou, G.-H.; Xu, X.-L. ROAV Method: A New Method for Determining Key Odor Compounds of Rugao Ham. *Food Sci.* **2008**, *29*, 370–374. [CrossRef]

25. Cao, Y.; Li, L. Improved protein-ligand binding affinity prediction by using a curvature-dependent surface-area model. *Bioinformatics* **2014**, *30*, 1674–1680. [CrossRef] [PubMed]
26. Eberhardt, J.; Santos-Martins, D.; Tillack, A.F.; Forli, S. AutoDock Vina 1.2.0: New Docking Methods, Expanded Force Field, and Python Bindings. *J. Chem. Inf. Model.* **2021**, *61*, 3891–3898. [CrossRef] [PubMed]
27. He, M.; Liu, W.; Zhang, C.; Liu, Y.; Zhuang, H.; O'Hagan, D. Selectively Fluorinated Citronellol Analogues Support a Hydrogen Bonding Donor Interaction with the Human OR1A1 Olfactory Receptor. *Org. Lett.* **2022**, *24*, 4415–4420. [CrossRef] [PubMed]
28. Ahmed, L.; Zhang, Y.; Block, E.; Buehl, M.; Corr, M.J.; Cormanich, R.A.; Gundala, S.; Matsunami, H.; O'Hagan, D.; Ozbil, M.; et al. Molecular mechanism of activation of human musk receptors OR5AN1 and OR1A1 by (R)-muscone and diverse other musk-smelling compounds [Biophysics and Computational Biology]. *Proc. Natl. Acad. Sci. USA* **2018**, *115*, E3950–E3958. [CrossRef] [PubMed]
29. Geithe, C.; Protze, J.; Kreuchwig, F.; Krause, G.; Krautwurst, D. Structural determinants of a conserved enantiomer-selective carvone binding pocket in the human odorant receptor OR1A1. *Cell. Mol. Life Sci.* **2017**, *74*, 4209–4229. [CrossRef] [PubMed]
30. Schmiedeberg, K.; Shirokova, E.; Weber, H.-P.; Schilling, B.; Meyerhof, W.; Krautwurst, D. Structural determinants of odorant recognition by the human olfactory receptors OR1A1 and OR1A2. *J. Struct. Biol.* **2007**, *159*, 400–412. [CrossRef] [PubMed]
31. Guo, X.; Ho, C.-T.; Wan, X.; Zhu, H.; Liu, Q.; Wen, Z. Changes of volatile compounds and odor profiles in Wuyi rock tea during processing. *Food Chem.* **2021**, *341*, 128230. [CrossRef] [PubMed]
32. Fan, Q.; Wang, X.; Zhao, Y.; Zheng, F.; Li, H.; Zhang, F.; Zhang, Y.; Chen, F. Characterization of key aroma compounds in Laobaigan Chinese Baijiu by GC×GC-TOF/MS and means of molecular sensory science. *Flavour Fragr. J.* **2019**, *34*, 514–525. [CrossRef]
33. Gemert, L.J. *Odour Thresholds: Compilations of Odour Threshold Values in Air, Water and Other Media*, 2nd ed.; Oliemans Punter & Partners BV: Zeist, The Netherlands, 2011.
34. Xu, Y.; Zhu, C.; Xu, C.; Sun, J.; Grierson, D.; Zhang, B.; Chen, K. Integration of Metabolite Profiling and Transcriptome Analysis Reveals Genes Related to Volatile Terpenoid Metabolism in Finger Citron (*C. medica* var. sarcodactylis). *Molecules* **2019**, *24*, 2564. [CrossRef] [PubMed]
35. Chi, P.T.L.; Van Hung, P.; Le Thanh, H.; Phi, N.T.L. Valorization of Citrus Leaves: Chemical Composition, Antioxidant and Antibacterial Activities of Essential Oils. *Waste Biomass Valori.* **2020**, *11*, 4849–4857. [CrossRef]
36. Jirapakkul, W.; Tinchan, P.; Chaiseri, S. Effect of drying temperature on key odourants in kaffir lime (*Citrus hystrix* D.C., Rutaceae) leaves. *Int. J. Food Sci. Technol.* **2013**, *48*, 143–149. [CrossRef]
37. Katsouli, E.; Panou, E.; Ziogas, V.; Ntamposi, E.; Graikou, K.; Chinou, I. Peel and Leaf Volatile Profiles of the New Citrus Hybrid 'Eugene' and Parent Species. *Horticulturae* **2025**, *11*, 1531. [CrossRef]
38. Vieira, D.D.S.S.; Emiliani, G.; Michelozzi, M.; Centritto, M.; Luro, F.; Morillon, R.; Loreto, F.; Gesteira, A.; Maserti, B. Polyploidization alters constitutive content of volatile organic compounds (VOC) and improves membrane stability under water deficit in Volkamer lemon (*Citrus limonia* Osb.) leaves. *Environ. Exp. Bot.* **2016**, *126*, 1–9. [CrossRef]
39. Azam, M.; Jiang, Q.; Zhang, B.; Xu, C.; Chen, K. Citrus Leaf Volatiles as Affected by Developmental Stage and Genetic Type. *Int. J. Mol. Sci.* **2013**, *14*, 17744–17766. [CrossRef] [PubMed]
40. Zahr, S.; Zahr, R.; El Hajj, R.; Khalil, M. Phytochemistry and biological activities of Citrus sinensis and Citrus limon: An update. *J. Herb. Med.* **2023**, *41*, 100737. [CrossRef]
41. Zheng, H.; Zhang, Q.; Quan, J.; Zheng, Q.; Xi, W. Determination of sugars, organic acids, aroma components, and carotenoids in grapefruit pulps. *Food Chem.* **2016**, *205*, 112–121. [CrossRef] [PubMed]
42. Cuevas, F.J.; Moreno-Rojas, J.M.; Ruiz-Moreno, M.J. Assessing a traceability technique in fresh oranges (*Citrus sinensis* L. Osbeck) with an HS-SPME-GC-MS method. Towards a volatile characterisation of organic oranges. *Food Chem.* **2017**, *221*, 1930–1938. [CrossRef] [PubMed]
43. Ling, Z.; Li, J.; Dong, Y.; Zhang, W.; Bai, H.; Li, S.; Wang, S.; Li, H.; Shi, L. Terpene produced by coexpression of the TPS and P450 genes from *Lavandula angustifolia* protects plants from herbivore attacks during budding stages. *BMC Plant Biol.* **2023**, *23*, 477. [CrossRef] [PubMed]
44. Lin, S.Y.; Roan, S.F.; Lee, C.L.; Chen, I.Z. Volatile organic components of fresh leaves as indicators of indigenous and cultivated citrus species in Taiwan. *Biosci. Biotechnol. Biochem.* **2010**, *74*, 806–811. [CrossRef] [PubMed]
45. Hijaz, F.; Nehela, Y.; Killiny, N. Possible role of plant volatiles in tolerance against huanglongbing in citrus. *Plant Signal. Behav.* **2016**, *11*, e1138193. [CrossRef] [PubMed]
46. Cheong, M.-W.; Loke, X.-Q.; Liu, S.-Q.; Pramudya, K.; Curran, P.; Yu, B. Characterization of Volatile Compounds and Aroma Profiles of Malaysian Pomelo (*Citrus grandis* (L.) Osbeck) Blossom and Peel. *J. Essent. Oil Res.* **2011**, *23*, 34–44. [CrossRef]
47. Jabalpurwala, F.A.; Smoot, J.M.; Rouseff, R.L. A comparison of citrus blossom volatiles. *Phytochemistry* **2009**, *70*, 1428–1434. [CrossRef] [PubMed]
48. Gardner, R.J. A property–activity approach to relating 'flavour' thresholds in one substrate to their value in a second substrate. *J. Sci. Food Agric.* **1981**, *32*, 146–152. [CrossRef] [PubMed]

49. Tandon, K.S.; Baldwin, E.A.; Shewfelt, R.L. Aroma perception of individual volatile compounds in fresh tomatoes (*Lycopersicon esculentum*, Mill.) as affected by the medium of evaluation. *Postharvest Biol. Technol.* **2000**, *20*, 261–268. [CrossRef]
50. Guo, Z.; Lu, Q.; Niu, Y.; Zhou, R.; Zhang, J.; Zhu, J.; Xiao, Z.; Qing, X. Molecular simulation analysis of differences in aroma synergy between three broad-spectrum proteins and four characteristic aroma compounds of sweet orange. *Food Biosci.* **2025**, *73*, 107713. [CrossRef]
51. Guo, L.; Li, W.; Zeng, J.; Zhu, Y.; Yan, H.; Zhang, Y.; Lv, H.; Lin, Z.; Yu, L.; Zhu, Y. Characterization of key odorants in three black tea cultivars using sensomics and molecular docking. *npj Sci. Food* **2026**. [CrossRef]
52. Li, C.-Z.; Wang, J.; Yang, J.-L. A comprehensive analysis combining E-nose, E-tongue, HS-GC-IMS, HS-GC-MS, and UPLC-QTOF-MS reveals the discriminatory aroma and numbness substances of *Zanthoxylum bungeanum* pericarps and pedicels. *Food Chem.* **2026**, *525*, 150384. [CrossRef] [PubMed]
53. Plotto, A.; Margaría, C.A.; Goodner, K.L.; Goodrich, R.; Baldwin, E.A. Odour and flavour thresholds for key aroma components in an orange juice matrix: Terpenes and aldehydes. *Flavour Fragr. J.* **2004**, *19*, 491–498. [CrossRef]
54. El Hadi, M.; Zhang, F.-J.; Wu, F.-F.; Zhou, C.-H.; Tao, J. Advances in fruit aroma volatile research. *Molecules* **2013**, *18*, 8200–8229. [CrossRef] [PubMed]
55. Ito, Y.; Kubota, K. Sensory evaluation of the synergism among odorants present in concentrations below their odor threshold in a Chinese jasmine green tea infusion. *Mol. Nutr. Food Res.* **2005**, *49*, 61–68. [CrossRef] [PubMed]
56. Hewson, L.; Hollowood, T.; Chandra, S.; Hort, J. Taste–aroma interactions in a citrus flavoured model beverage system: Similarities and differences between acid and sugar type. *Food Qual. Prefer.* **2008**, *19*, 323–334. [CrossRef]

Disclaimer/Publisher's Note: The statements, opinions and data contained in all publications are solely those of the individual author(s) and contributor(s) and not of MDPI and/or the editor(s). MDPI and/or the editor(s) disclaim responsibility for any injury to people or property resulting from any ideas, methods, instructions or products referred to in the content.